The main perturbing objects on the orbits of (616) Prometheus and (617) Pandora

A. R. Gomes-Júnior, T. Santana, O. C. Winter, R. Sfair

Monthly Notices of the ROYAL ASTRONOMICAL SOCIETY

MNRAS **511,** 4842–4849 (2022) https://doi.org/10.1093/mnras/stac330
Advance Access publication 2022 February 8

The main perturbing objects on the orbits of (616) Prometheus and (617) Pandora

A. R. Gomes-Júnior [1,2]★ T. Santana [1,4]★ O. C. Winter [1] and R. Sfair [1,3]

[1] *UNESP – São Paulo State University, Grupo de Dinâmica Orbital e Planetologia, Guaratinguetá 12516-410, SP, Brazil*
[2] *Laboratório Interinstitucional de e-Astronomia – LIneA, Rua Gal. José Cristino 77, Rio de Janeiro 20921-400, RJ, Brazil*
[3] *Institut für Astronomie und Astrophysik, Eberhard Karls Universität Tübingen, Auf der Morgenstelle 10, D-72076 Tübingen, Germany*
[4] *LESIA, Observatoire de Paris, 5 place Jules Janssen, 92195 Meudon, France*

Accepted 2022 February 3. Received 2022 February 1; in original form 2021 December 20

ABSTRACT

The dynamical evolution of the Prometheus and Pandora pair of satellites is chaotic, with a short 3.3 yr Lyapunov time. It is known that the anti-alignment of the apses line of Prometheus and Pandora, which occurs every 6.2 yr, is a critical configuration that amplifies their chaotic dynamical evolution. However, the mutual interaction between Prometheus and Pandora is not enough to explain the longitudinal lags observed by the *Hubble Space Telescope*. The main goal of the current work is to identify the main contributors to the chaotic dynamical evolution of the Prometheus–Pandora pair beyond themselves. Therefore, in this work, we first explore the sensibility of this dynamical system to understand it numerically and then build numerical experiments to reach our goals. We identify that almost all major satellites of the Saturn system play a significant role in the evolution of Prometheus's and Pandora's orbits.

Key words: methods: numerical – celestial mechanics – planets and satellites: individual: Pandora – planets and satellites: individual: Prometheus.

1 INTRODUCTION

Observations made during the ring plane crossing of 1995 by the *Hubble Space Telescope* (*HST*) revealed that the angular positions of Prometheus and Pandora were shifted from the expected values (Bosh & Rivkin 1996; Nicholson et al. 1996; McGhee 2000). The accepted explanation for the lags is the chaotic orbital evolution associated with a mean motion resonance between the two satellites (Goldreich 2003; Goldreich & Rappaport 2003; Renner & Sicardy 2005). However, the values of the ratio between the lags of Prometheus and Pandora along the time clearly show that the mutual interaction between the two satellites is far from being enough to explain the measured angular gaps (Santana, Winter & Mourão 2020).

A few works performed simulations including other satellites. For example, French et al. (2003) determined with high precision the astrometric positions of Prometheus, Pandora, and nine other satellites using a large set of images taken by the Wide Field and Planetary Camera of the *HST* from 1996 to 2002. By comparing the data from the expected positions, the authors computed mean longitudes and lags for the pair of satellites. They proposed that a resonance involving the F ring could be the common origin of the uncertainty of their positions.

Cooper & Murray (2004) performed numerical simulations of the full equations of motion to study the orbits of Prometheus and Pandora over 30 yr under the presence of the eight major satellites of Saturn's system (Mimas, Enceladus, Tethys, Dione, Rhea, Titan, Hyperion, and Iapetus), plus the pair Janus and Epimetheus. The authors confirmed that the anticorrelation in the temporal variation of the two satellites' mean longitudes remains maintained when the others are considered. They also confirmed the chaos on Prometheus's orbit by computing its Lyapunov exponent, while for Pandora, it was implied by the sensibility of the initial conditions used in the simulations. Moreover, through theoretical analysis, a role for the pair Janus and Epimetheus through two second-order eccentricity mean motion resonances, 17:15 and 21:19, is also pointed out as important for the chaotic behaviour of Prometheus and Pandora, but on a longer time-scale.

In Renner, Sicardy & French (2005), the authors fitted numerical simulations also within the *HST* data. Using a Radau integrator, the system consisted of the major satellites of the Saturn system: Epimetheus, Janus, Mimas, Enceladus, Tethys, Dione, Rhea, Titan, and Iapetus, and allowed the authors to confirm the chaotic behaviour of Prometheus and Pandora. Furthermore, they also derived the masses and densities of the satellites. The authors state that the chaotic interaction between Prometheus and Pandora remains in the addition of the other satellites. They also point out the influence of Mimas through the nearby corotation resonance 3:2 with Pandora, and the Janus and Epimetheus dynamical influence as well, in agreement with Cooper & Murray (2004).

The current work aims to identify the main contributors to the chaotic dynamical evolution of the Prometheus–Pandora system beyond themselves. However, the high instability of the system is a major difficulty in reaching our goal. Therefore, in this work, we first explore the sensibility of this dynamical system to understand it numerically and then build up numerical experiments that allow us to identify each of the bodies that significantly contribute to the chaotic behaviour of Prometheus and Pandora.

★ E-mail: altairgomesjr@gmail.com (AJ); t.santana@unesp.br (TS)

The work can be divided into three parts. The first one is devoted to better understanding the high sensibility of the Prometheus–Pandora system by comparing our models with the NASA Jet Propulsion Laboratory (JPL) ephemeris (Acton 1996).

The second part is concerned with the strong instability generated by the anti-alignment of the apses line of Prometheus and Pandora, which occurs periodically. Any slight orbital difference is significantly amplified during one of these anti-alignments. Consequently, after a few anti-alignments, the angular difference might drastically increase.

The third and last part of this work focuses on identifying Saturn's satellites that are relevant for the chaotic evolution of Prometheus and Pandora, beyond that generated by their mutual interaction (including the effect due to the near 3:2 mean motion resonance between Mimas and Pandora).

Therefore, Section 2 describes the approach adopted in the numerical integration of the satellites' orbits. In Section 3, we will present the numerical integrations considering 20 objects of the Solar system with different epochs for initial conditions to fit our model to the JPL ephemeris. Section 4 will numerically verify the anti-alignment implications when studying the orbits of Prometheus and Pandora. Section 5 will present our numerical experiments, which reveal the more relevant satellites on the dynamical evolution of the Prometheus–Pandora pair. Then, in Section 6 we will provide our final comments.

2 METHODOLOGY

Using our software, named BOSS (Brazilian Orbital Solution for Satellites), we integrate the equations of motion to determine the dynamical evolution of the orbits of Prometheus and Pandora. The numerical model of Saturn's satellites is in a Saturncentric reference frame with axes in the International Celestial Reference System (ICRS/J2000). The equations of motion are presented in equation (1) and described in Lainey, Duriez & Vienne (2004a).

$$\ddot{\boldsymbol{r}}_i = -G(M_\mathrm{S}+m_i)\frac{\boldsymbol{r}_i}{r_i^3} + \sum_{j=1}^{N} Gm_j\left(\frac{\boldsymbol{r}_j-\boldsymbol{r}_i}{r_{ij}^3} - \frac{\boldsymbol{r}_j}{r_j^3}\right) + G(M_\mathrm{S}+m_i)\nabla U_{\bar{i}\hat{S}} + \sum_{j=1}^{N} Gm_j\nabla U_{\bar{j}\hat{S}}, \quad (1)$$

where

$$\begin{aligned} U_{\bar{i}\hat{S}} = &-\frac{R_\mathrm{S}^2 J_2}{r_i^3}\left(\frac{3}{2}\sin^2\Phi_i - \frac{1}{2}\right) \\ &-\frac{R_\mathrm{S}^3 J_3}{r_i^4}\left(\frac{5}{2}\sin^3\Phi_i - \frac{3}{2}\sin\Phi_i\right) \\ &-\frac{R_\mathrm{S}^4 J_4}{r_i^5}\left(\frac{35}{8}\sin^4\Phi_i - \frac{15}{4}\sin^2\Phi_i + \frac{3}{8}\right) \\ &-\frac{R_\mathrm{S}^6 J_6}{r_i^7}\left(\frac{231}{16}\sin^6\Phi_i - \frac{315}{16}\sin^4\Phi_i \right. \\ &\left. +\frac{105}{16}\sin^2\Phi_i - \frac{5}{16}\right) \end{aligned} \quad (2)$$

with the following notation:

(i) S stands for Saturn and corresponding mass M_S and radius R_S;

(ii) i stands for the satellite whose equations of motion are being considered, its mass m_i and position relative to Saturn $\boldsymbol{r}_i$, with the respective distance r_i;

Table 1. Dynamical constants from SAT393 used in the model (see Section 2).

Constant	Value	Unit
Janus GM	1.265 765 099 012 197E−01	$km^3\ s^{-2}$
Epimetheus GM	3.512 333 288 208 074E−02	$km^3\ s^{-2}$
Helene GM	3.424 829 447 502 984E−04	$km^3\ s^{-2}$
Atlas GM	3.718 871 247 516 475E−04	$km^3\ s^{-2}$
Prometheus GM	1.075 208 001 007 610E−02	$km^3\ s^{-2}$
Pandora GM	9.290 325 122 028 795E−03	$km^3\ s^{-2}$
Mimas GM	2.503 629 609 027 271E−00	$km^3\ s^{-2}$
Hyperion GM	3.712 505 242 740 757E−01	$km^3\ s^{-2}$
Phoebe GM	5.533 878 663 162 022E−01	$km^3\ s^{-2}$
Enceladus GM	7.210 841 599 764 501E+00	$km^3\ s^{-2}$
Tethys GM	4.120 864 966 231 671E+01	$km^3\ s^{-2}$
Dione GM	7.311 562 440 698 799E+01	$km^3\ s^{-2}$
Iapetus GM	1.205 075 311 030 973E+02	$km^3\ s^{-2}$
Rhea GM	1.539 433 320228564E+02	$km^3\ s^{-2}$
Titan GM	8.978 137 712 627 313E+03	$km^3\ s^{-2}$
Jupiter system GM	1.267 127 641 000 000E+08	$km^3\ s^{-2}$
Uranus system GM	5.794 556 400 000 000E+06	$km^3\ s^{-2}$
Neptune system GM	6.836527100580000E+06	$km^3\ s^{-2}$
Sun GM	1.327 132 332 639 221E+11	$km^3\ s^{-2}$
Saturn GM	3.793 120 655 618 811E+07	$km^3\ s^{-2}$
Sat. J_2	1.629 133 249 525 738E−02	
Sat. J_3	1.494 723 182 852 077E−06	
Sat. J_4	−9.307 138 534 779 719E−04	
Sat. J_6	8.943 208 329 411 604E−05	
Sat. equatorial radius	60 330	km
Sat. pole α_p	40.5839	deg
Sat. pole rate $\dot{\alpha}_\mathrm{p}$	−0.050 58	$^\circ$ $century^{-1}$
Sat. pole δ_p	83.5377	deg
Sat. pole rate $\dot{\delta}_\mathrm{p}$	−0.005 53	deg $century^{-1}$
Sat. prime meridian angle	38.9	deg
Sat. rotation rate	810.793 90	deg d^{-1}

(iii) j corresponds to any of the other N bodies of the Solar system that are perturbing i: other satellites, the planets (except Saturn), and the Sun. m_j is the corresponding mass. $\boldsymbol{r}_j$ and r_j are the position and distance relative to Saturn, respectively;

(iv) r_{ij} is the distance between the bodies i and j;

(v) $U_{\bar{i}\hat{S}}$ and $U_{\bar{j}\hat{S}}$ are the gravitational potential caused by the oblateness of Saturn experienced by body i and j, respectively;

(vi) J_2, J_3, J_4, and J_6 are zonal harmonic coefficients of Saturn's gravitational potential of second, third, fourth, and sixth order, respectively;

(vii) Φ_i is the latitude of the body i in the Saturnian equatorial frame.

For the analysis described in Sections 3–5, different sets of dynamical constants and perturbers will be used. For every case, the values of these constants are the same as the JPL kernel SAT393.[1] Table 1 presents the values for the dynamical constants used in our models extracted from SAT393.

The equations of motion are integrated using the 15th-order integrator Gauss-Radau (Everhart 1985) with a constant step of 0.025 d. Unless stated otherwise, for each simulation, only the orbits of Prometheus and Pandora are being integrated, while the positions of the perturbing objects come from the ephemeris and are not being redetermined.

[1] https://naif.jpl.nasa.gov/pub/naif/generic_kernels/spk/satellites/sat393.cmt

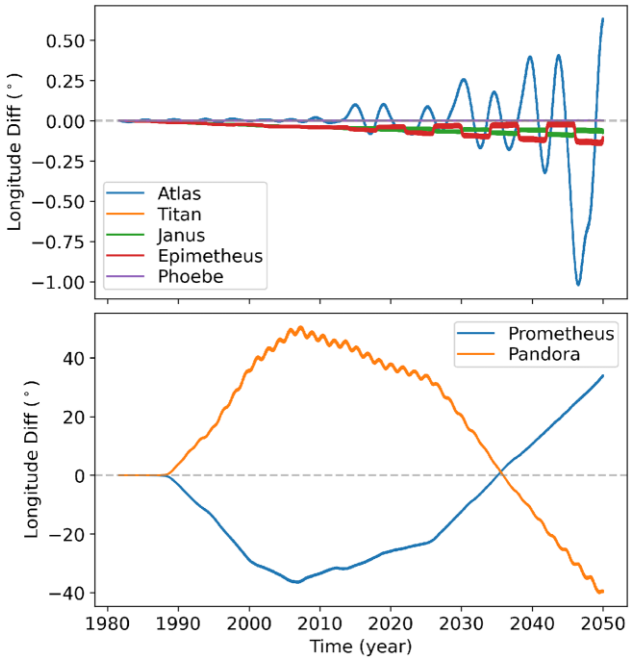

Figure 1. Difference in true longitude between BOSS and JPL SAT393 in integrations where only the referred satellite was integrated and all the perturbers' positions come from the ephemeris.

3 ON THE ORBITS OF PROMETHEUS AND PANDORA

The JPL ephemeris SAT393 was fitted to the observations obtained from 1980 up to 2016. In this period, many observations of Prometheus and Pandora were obtained by the *Voyager I* and *II* spacecraft, the *HST*, and, mainly, by the *Cassini* spacecraft (Cooper et al. 2015).

Our initial goal was to fit our model to the observations. However, a large set of astrometric positions is not publicly available. For instance, the Natural Satellites Database[2] (Arlot & Emelyanov 2009) of Paris Observatory only contains positions from *Cassini* up to 2013 and none from the *Voyagers*. Therefore, determining the astrometry of these satellites from the observations is out of the scope of this work.

Because of that, we will use the ephemeris from the SAT393 kernel to represent the observations. In this regard, we first try to replicate the SAT393 model by using the same constants and initial conditions. In this case, we used all the objects described in Table 1 in the numerical model. The integration was realized between 1981, near *Voyager II*'s closest approach to Saturn, and 2050, the limit of the SAT393 ephemeris. The positions for all perturbers come from the ephemeris itself.

The same test was applied for other objects of the Saturn system to see their behaviour compared with Prometheus and Pandora: Atlas, Titan, Phoebe, and the pair Janus–Epimetheus. Then, we compared the difference in true longitude between BOSS and SAT393, as shown in Fig. 1.

The results show that our model retrieved well the orbits of Atlas, Titan, Phoebe, and the pair Janus–Epimetheus. In the period studied, the difference in longitude was smaller than 1° for Atlas, which is probably due to its 54:53 mean motion resonance with Prometheus, and smaller than 0.2° for Titan, Janus–Epimetheus, and Phoebe. Up to the last observations by *Cassini*, in 2016, the difference is smaller than 0.2° for all satellites.

However, the same test for Prometheus's and Pandora's orbits showed a difference of up to 40° in true longitude. This difference was reached ∼25 yr after the beginning of the integration. The more considerable difference observed in Prometheus and Pandora relative to the smaller ones observed with the other satellites confidently tells us this difference is mainly caused by a dynamical interaction rather than a numerical error.

Four other simulations, starting at different epochs (J1985, J1991, J2001, and J2020) and ending in J2050, were also made. These epochs were randomly chosen to verify the behaviour due to different spatial configurations as initial conditions. In all these cases, the difference in true longitude for Prometheus and Pandora between SAT393 and BOSS was still huge, with the maximum difference varying between 20° and 100°. Furthermore, the behaviour of these differences largely varies depending on the initial epoch.

Finally, we tried to force our model on the orbits of Prometheus and Pandora to be the same as the SAT393 in the period of observations. With this, we expect to have a model indirectly fitted to the *observations* where the parameters can be later changed to study its behaviour. For that, we generated positions of both satellites from the SAT393 ephemeris uniformly distributed in the interval 1980–2020 and used them as *observations* to be fitted in our model. The positions of the perturbing satellites were obtained directly from the SAT393 model; thus, their orbits were not being integrated, as described in Section 2. In this case, the initial conditions were from SAT393 at the epoch J2000, the middle of the chosen interval.

The process of fitting is described in Lainey, Arlot & Vienne (2004b). First, the variational equations of the force function relative to the initial conditions are simultaneously integrated with equation (1). Then, these equations are fitted to the offset between the observations and the numerical model using a least-squares method, resulting in new initial conditions.

The fit did not converge when we used all the positions directly. To avoid it, we used only a few observations close to the initial epoch, fitted new initial conditions, and then repeated the process, increasing the *observations* for a larger interval of time.

The difficulty of fitting the orbits of Prometheus and Pandora, using all the intervals of observations, from *Voyager I* to *Cassini* is a common issue (Lainey, 2020, private communication). Usually, different models are fitted, where each one is suitable for a different interval of time. We were able to fit our model to the SAT393 ephemeris using points distributed over the period 1983 and 2017. Further than that, even with a slight increase in the interval of the ephemeris considered, the fit diverges again.

Fig. 2 shows the difference between BOSS and SAT393 after we have fitted a numerical model to the SAT393 ephemeris between J1983 and J2017. The residuals are mostly of the order of 10 km, with 30 km in the extremities of the interval. The differences in initial conditions are of the order of 1 km.

All these tests showed how sensitive the orbits of Prometheus and Pandora are. Unfortunately, their chaotic behaviour prevents us from propagating their trajectories for more than a few years reliably. Therefore, observations must be obtained more frequently than for other satellites of the Saturn system to keep track of their spatial motion.

4 THE ANTI-ALIGNMENT

Goldreich & Rappaport (2003) showed that Prometheus and Pandora have a close approach every 6.2 yr when an anti-alignment of their orbits' apses happens. Furthermore, they showed that these events,

[2]http://nsdb.imcce.fr/obspos/obsindhe.htm

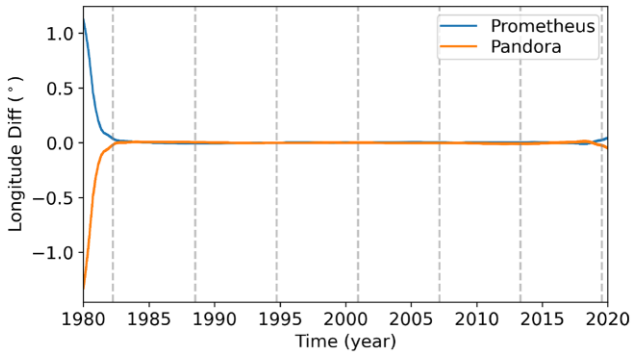

Figure 2. Difference in true longitude between the numerical model obtained from the fitting to the SAT393 ephemeris using BOSS and SAT393 itself. The dashed lines are the anti-alignment between Prometheus and Pandora discussed in Section 4.

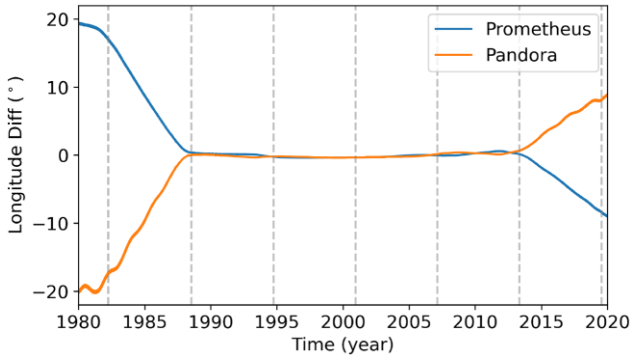

Figure 3. Difference in true longitude between BOSS and SAT393 starting an integration forward and backward in time during the anti-alignment of 2000 December. Each vertical dashed line marks an anti-alignment between the orbits of Prometheus and Pandora.

which occurred ∼0.61, 6.9, 13.1, and 19.3 y after *Voyager II*'s closest approach to Saturn in August 1981, are one of the sources of their chaotic motion.

In Fig. 1, we notice that the difference between the models remained smaller than 0.2° and started to grow after 6 yr from the initial epoch, in contrast with the Lyapunov time of ∼3.3 yr reported by Cooper & Murray (2004). In other words, we found regions where the trajectory is well behaved for twice the Lyapunov time. Probably, the reason is that we started the integration close to the 1982 anti-alignment, while the model diverged near the 1988 anti-alignment. In comparison, the Lyapunov exponent is calculated for a period long enough to cross many anti-alignments.

We performed simulations using initial conditions on the epochs of anti-alignment. The intention is to minimize the difference to SAT393 of this specific event and maximize the interval without another close encounter. We also included the anti-alignments at 25.5, 31.7, and 37.9 yr after the referred epoch and an integration starting at the symbolic epoch J2000.

In each of these simulations, the integration was done backward up to 1980 and forwarded up to 2020 with an output every day. All of the complete set of constants shown in Table 1 was used.

Fig. 3 shows an integration started in the anti-alignment of 2000 December. We note that the first anti-alignment before and after the initial epoch, respectively in 1994 and 2007, does not produce any significant divergence between our model and SAT393. Only when close to the second closest approach, in 1988 and 2013, does the model start to diverge. Between these epochs, the difference grows linearly, showing only a small difference in the semimajor axis.

In Appendix A, we present the difference between BOSS and SAT393 from integrations starting at different anti-alignments. We note there is no visual pattern between these tests. However, in most cases, we can still recover the orbits of Prometheus and Pandora between the starting epoch and the subsequent anti-alignment. For the case shown in Fig. 3, the trajectories are recovered for almost two close encounters.

As stated in Section 1, we are most interested in identifying the main contributors to the chaotic dynamical evolution of Prometheus and Pandora beyond themselves. It is clear from Fig. 3, and also from Fig. 2, that, to achieve our goals, we should analyse the orbits between two consecutive anti-alignments, where the chaotic motion caused by a close encounter is reduced.

5 THE RELEVANT SATELLITES

Cooper & Murray (2004) already have studied the dynamical influence of the Saturnian satellites. However, although they notice the importance of Titan and Janus–Epimetheus, they do not discuss the significance of the other satellites on the orbits of Prometheus and Pandora.

Our final analysis consisted of verifying the objects that most affect Prometheus's and Pandora's orbits in an interval between two consecutive closest approaches. For this, we built an experiment to emphasize the direct perturbation of each test object: First, we integrate the orbits of Prometheus and Pandora using the complete set of objects present in Table 1 as a base model; then an integration is made removing the test object from the list; and finally, the difference in true longitude to the base model is computed.

In this experiment, the direct influence of the tested perturbing object does not affect Prometheus and Pandora, as the object is removed from the system. However, as explained in Section 2, the orbits of the remaining perturbing objects come directly from the SAT393 model, which in turn were determined considering the object we are removing. Thus, the indirect perturbation of the removed object is still preserved in our simulations.

We verified the dynamical perturbations on Prometheus and Pandora caused by all the bodies present in SAT393 whose masses are known: the Sun, the Giant Planets, Enceladus, Tethys, Dione, Rhea, Titan, Mimas, the pair Janus–Epimetheus, Helene, Atlas, Hyperion, Iapetus, and Phoebe. These integrations were done in an interval of 5 yr between two consecutive anti-alignments in four distinct periods covering the epochs of the ring plane crossing and the *Cassini* observations: 1995–2000, 2001–2006, 2007–2012, and 2013–2018. As a basis for comparison, we also integrated the orbit of Prometheus without the direct perturbation of Pandora and vice versa.

Table 2 and Fig. 4 show the maximum difference in true longitude for Prometheus and Pandora caused by the exclusion of each test object in each period considered. The difference is in the sense model with minus the model without the object, i.e. base model minus model without the object.

First of all, it is clear that the planets, the Sun, and the satellites Hyperion, Iapetus, Phoebe, and Helene are not significant for the orbits of Prometheus and Pandora. This is expected since they are the smallest or the most distant objects from these satellites.

For the case of Mimas, it is known that the near 3:2 resonance with Pandora is of major importance (Evans 2001). In fact, in our tests, the difference in longitude of Pandora caused by Mimas was always more prominent than that caused by Prometheus reaching $\Delta\lambda$

Table 2. Maximum difference in true longitude in the orbits of the Saturnian satellites Prometheus and Pandora when the direct perturbation of a body is ignored. The variations were computed in intervals between two consecutive anti-alignments.

Perturber	Sat.	1995–2000	2001–2006	2007–2012	2013–2018
Mimas	Pro	+0.17	−2.75	+2.60	−0.56
	Pan	−4.79	−8.98	−15.85	−12.95
Prometheus	Pan	2.69	0.28	−4.47	2.48
Pandora	Pro	−1.98	−0.33	3.62	−1.70
Enceladus	Pro	−0.18	−0.10	−0.14	−0.19
	Pan	−0.18	−0.17	−0.16	−0.25
Tethys	Pro	−0.06	−0.36	−0.30	−0.33
	Pan	−0.06	−0.18	−0.44	−0.48
Dione	Pro	−0.17	−0.12	−0.24	−0.35
	Pan	+0.22	+0.05	−0.33	−0.45
Rhea	Pro	+0.06	−0.15	−0.14	−0.14
	Pan	−0.13	−0.24	−0.15	+0.05
Titan	Pro	−0.49	−0.31	+1.43	−0.28
	Pan	−0.32	−0.79	−2.25	+0.20
Janus–Epimetheus	Pro	−0.49	+0.36	−0.30	+0.15
	Pan	−0.61	−0.16	−0.15	+0.40
Atlas	Pro	−0.36	+0.22	+0.15	−0.14
	Pan	−0.28	+0.11	+0.06	−0.07
Hyperion	Pro	-8×10^{-6}	-1×10^{-5}	-1×10^{-5}	-1×10^{-5}
	Pan	$+9 \times 10^{-6}$	-1×10^{-5}	-8×10^{-6}	-2×10^{-5}
Iapetus	Pro	-4×10^{-4}	$+1 \times 10^{-4}$	-1×10^{-4}	-4×10^{-4}
	Pan	-4×10^{-4}	$+2 \times 10^{-4}$	-3×10^{-4}	-2×10^{-4}
Phoebe	Pro	-3×10^{-8}	$+1 \times 10^{-8}$	-6×10^{-8}	$+1 \times 10^{-8}$
	Pan	-6×10^{-8}	$+2 \times 10^{-8}$	-1×10^{-7}	$+5 \times 10^{-8}$
Helene	Pro	$+5 \times 10^{-7}$	-5×10^{-7}	-2×10^{-7}	$+2 \times 10^{-7}$
	Pan	-1×10^{-6}	-1×10^{-6}	-3×10^{-7}	-5×10^{-7}
Sun	Pro	-7×10^{-3}	$+3 \times 10^{-3}$	-5×10^{-3}	-6×10^{-3}
	Pan	-6×10^{-3}	$+2 \times 10^{-3}$	-8×10^{-3}	-6×10^{-3}
Jupiter	Pro	-5×10^{-6}	$+2 \times 10^{-5}$	-2×10^{-6}	-3×10^{-6}
	Pan	-6×10^{-6}	$+4 \times 10^{-5}$	-2×10^{-6}	-4×10^{-6}
Uranus	Pro	$+5 \times 10^{-8}$	-5×10^{-8}	-5×10^{-8}	-5×10^{-8}
	Pan	-7×10^{-8}	-7×10^{-8}	-8×10^{-8}	-9×10^{-9}
Neptune	Pro	-2×10^{-8}	-4×10^{-8}	-7×10^{-8}	-2×10^{-8}
	Pan	-5×10^{-8}	-2×10^{-8}	-8×10^{-8}	$+3 \times 10^{-8}$

$\sim 15^\circ$ in the interval 2007–2012. The difference in the longitude of Prometheus' orbit caused by Mimas was smaller than 3° ($\Delta\lambda \sim 5^\circ$) and was more significant than the perturbation caused by Pandora only in the interval 2001–2006.

For the remaining satellites, their dynamical influences are of the foremost importance but much less significant than that of Mimas. The variation over time can be seen in Fig. 5 and the maximum difference reached in each interval is summarized in Table 2.

First, we notice that, in the majority of the cases, the variation in true longitude in Prometheus and Pandora caused by the missing of a specific perturber is in the opposite direction for each other. It is interesting to note that while the missing of Mimas caused a lag in the orbit of Prometheus in 2001–2006, Prometheus would be ahead of its expected position in 2007–2012 by almost the same amount.

For Enceladus, the absence of its direct perturbation caused a lag of $\sim 0.2^\circ$ in both satellites regardless of the epoch studied. Without Tethys, almost no lag was identified in 1995–2000, but a lag of nearly 0.5° was identified in 2013–2018. For Dione, the period 2013–2018 is also when it would cause the most considerable lag ($\sim 0.4^\circ$) in the orbits of Prometheus and Pandora. For Rhea, the lags are consistent in all the intervals, with variations smaller than 0.25°.

The missing of the direct perturbation of Titan caused a lag of 2.25° in the orbit of Pandora, and a lead of 1.43° in the orbit of Prometheus, in the interval 2007–2012. During this period, only Mimas was more important than Titan. In the interval 2001–2006, the perturbation of Titan on Pandora was also more significant than that caused by Prometheus. However, in the interval 2013–2018, the direct perturbation of Titan is less important than Mimas, Tethys, and Dione.

The pair Janus–Epimetheus also contributes to Prometheus's and Pandora's orbital evolution. Cooper & Murray (2004) showed that when Epimetheus switches its orbit with Janus, the 17:15 eccentricity resonance sweeps across Prometheus's orbit. At the same time, the 21:19 eccentricity resonance sweeps across Pandora's orbit. The direct perturbation of Janus–Epimetheus was found to be the second most crucial interaction with Prometheus and Pandora in the period 1995–2000 ($\Delta\lambda \sim 0.6^\circ$), but similar to the perturbation by other objects in the remaining periods tested.

Atlas has also been identified as having mean motion resonances 54:53 with Prometheus and 70:67 with Pandora by Spitale et al. (2006). Thus, in our simulations, the direct perturbation of Atlas affects Prometheus more than Pandora. However, in the periods tested, the perturbation of Atlas is not higher than that caused by other satellites.

6 FINAL COMMENTS

The dynamics of the orbits of Prometheus and Pandora is very complex. After the discovery, their orbits presented longitudinal lags from the expected positions as observed by the *Hubble Space Telescope* during the Ring Plane Crossing (Evans 2001). Furthermore, a chaotic behaviour associated with a 121:118 mean motion resonance was found responsible for the lags as described by Goldreich (2003). Because of it, an anti-alignment of the orbits of these satellites happens every 6.2 yr, amplifying their chaotic dynamical evolution. However, as pointed out by Santana et al. (2020), the mutual interaction between Prometheus and Pandora alone is not enough to explain the observed lags. In this regard, we realized a study of the orbits of Prometheus and Pandora in an attempt to identify the bodies that could potentially contribute to their chaotic motion.

To study the period covered by the observations from *Voyager I* (1980) until *Cassini* (2016), we used the JPL SAT393 ephemeris as a comparative. In an attempt to replicate the SAT393 ephemeris, using the same dynamical parameters and the ephemeris itself as initial conditions, our model quickly diverged from the ephemeris. At the same time, our model managed to replicate the orbits of Atlas, Titan, Janus–Epimetheus, and Phoebe. Unfortunately, we could not reliably propagate the orbits of Prometheus and Pandora for more than a few years, even when we forced our model to be the same as the SAT393 ephemeris. This shows how sensitive their orbits are.

Our model only diverged from the SAT393 one once Prometheus's and Pandora's orbits were close to the anti-alignment. To minimize the effects of a specific anti-alignment and maximize the interval without experiencing another one, we made simulations starting at these epochs. We notice that the difference between the models started when crossing to the first anti-alignment. In one particular case, 2000 December, shown in Fig. 3, only the second anti-alignment was able to cause a significant divergence between our model and the SAT393, while the difference in true longitude between two consecutive anti-alignments grows linearly, meaning a difference in the semimajor axis. As expected, the anti-alignment between

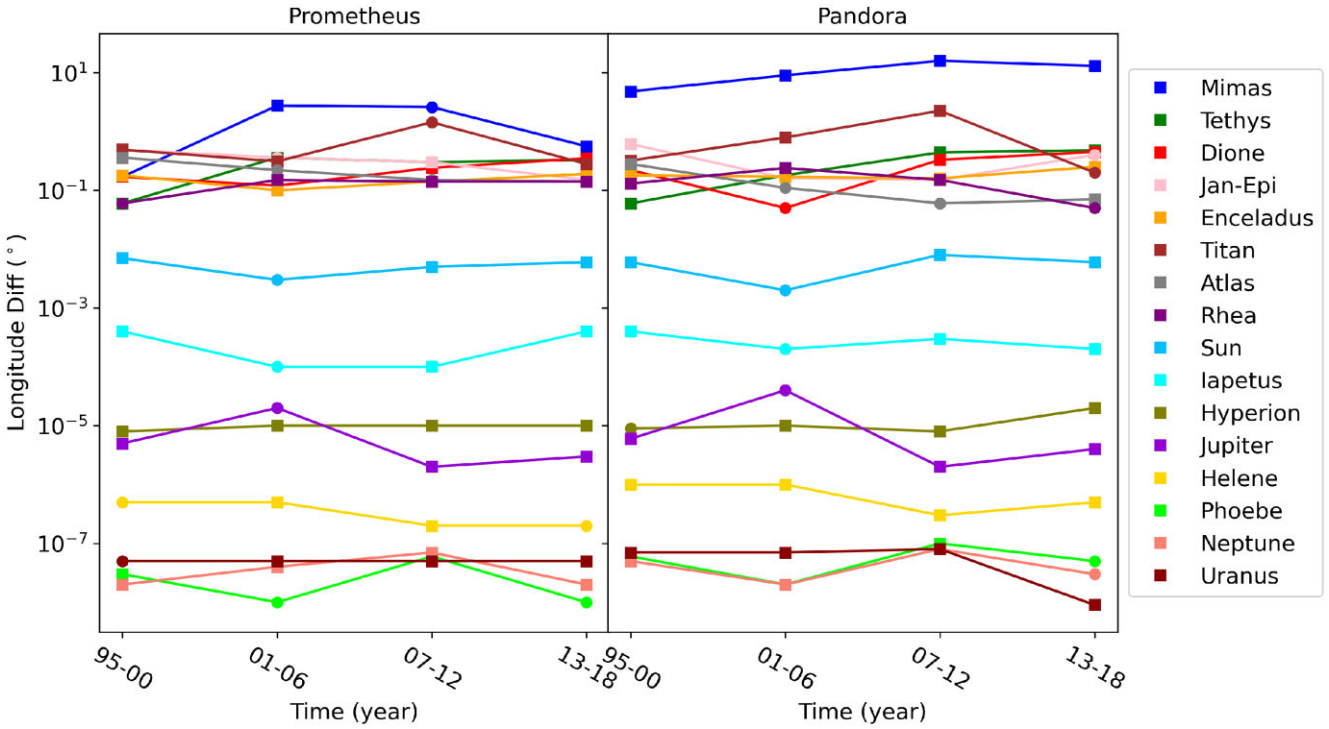

Figure 4. Visual representation of Table 2. Each point is the maximum absolute difference in the true longitude of the orbits of Prometheus and Pandora caused by the presence of a specific perturbing object. Square points represent the negative values (lag), while the dots represent the positive ones (ahead).

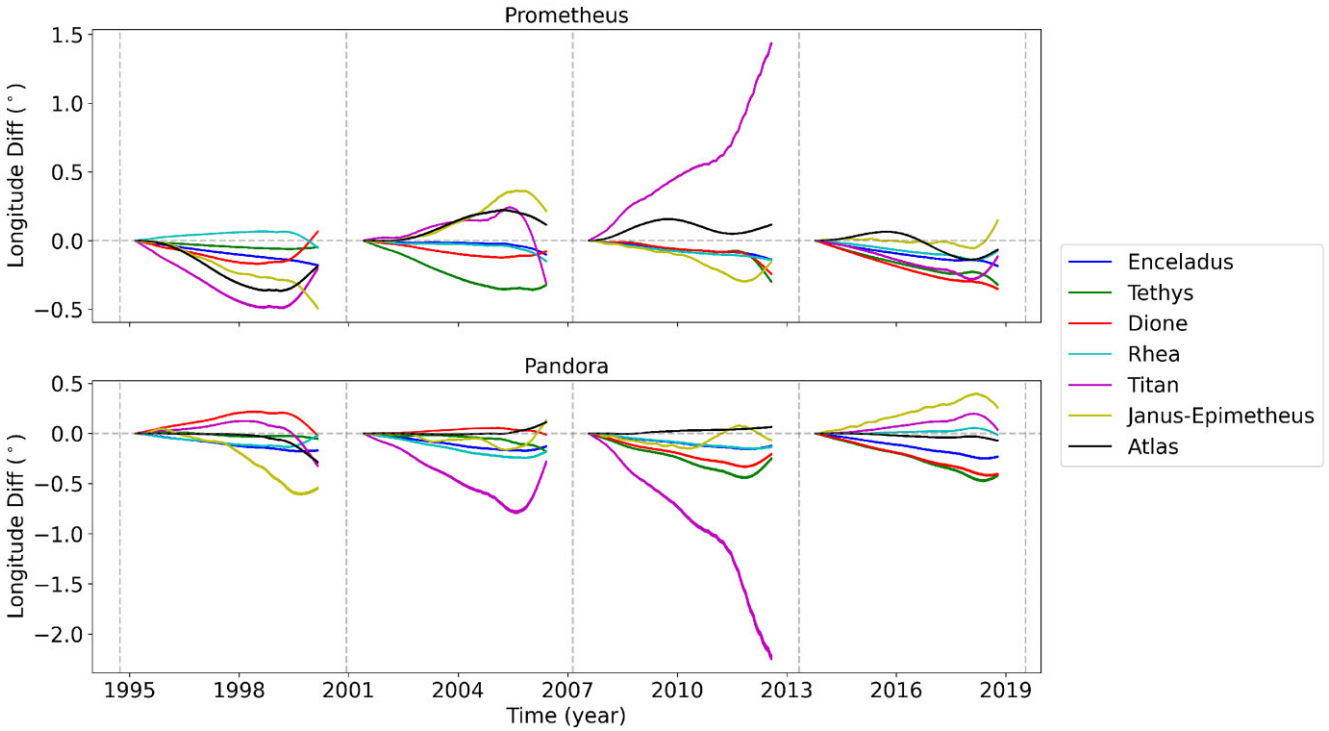

Figure 5. Difference in true longitude between BOSS and SAT393 for integrations where a specific perturber was removed compared with the one where all perturbers were considered. The variation caused by the absence of Mimas is not shown as it is much larger than the others.

Prometheus and Pandora is the leading cause of the instability of their orbits. We were able to replicate the SAT393 model for a period of ∼6 yr in almost all our tests, compared to the Lyapunov time of 3.3 yr.

Finally, to identify the essential satellites to reproduce the motions of Prometheus and Pandora, we made numerical integrations between two consecutive anti-alignments. In this interval, we minimize the importance of the closest encounters, which better show us other

effects. Furthermore, the tests were made comparing a simulation without a specific satellite and an orbit where all satellites were present, thus considering only the direct perturbation of the satellites.

These simulations showed us that Mimas, Enceladus, Tethys, Dione, Rhea, Titan, Janus–Epimetheus, and Atlas seemed to be of utmost importance for the orbits of Prometheus and Pandora. All of them could cause a variation in the longitude of Prometheus's and Pandora's orbits of $\sim 0.2^{\circ}$, which will be amplified when crossing an anti-alignment. Thus, we conclude that any model that intends to study the trajectories of Prometheus and Pandora should consider at least these nine satellites.

Quillen & French (2014) analysed the three-body resonances in the Uranian satellite system in an attempt to identify theoretically and numerically which types of three-body resonances might be important. Our work was focused on the numerical simulations of Prometheus's and Pandora's orbits in the context of the observations from *Voyager I*, in 1980, up to *Cassini*, in 2016. Thus, we do not discuss unknown resonances that could explain the results obtained. However, we encourage further analysis to look for possible three-body resonances in the system, in view of a large number of known two-body resonances associated with both satellites: Prometheus–Pandora 121:118 mean motion resonance; Mimas–Pandora 3:2 corotation resonance, which, in turn, it is known that Mimas is in a 2:1 mean motion resonance with Tethys; Epimetheus–Prometheus and Epimetheus–Pandora 17:15 and 21:19 eccentricity resonances, respectively, with Epimetheus in corotation with Janus; and Atlas–Prometheus and Atlas–Pandora 54:53 and 70:67 mean motion resonances, respectively .

ACKNOWLEDGEMENTS

The authors acknowledge the respective grants: São Paulo Research Foundation (FAPESP, proc. 2016/24561-0 and 2018/11239-8), Brazilian National Council for Scientific and Technological Development (CNPq, proc. 305210/2018-1), the Brazilian Federal Agency for Support and Evaluation of Graduate Education (CAPES), in the scope of the Program CAPES-PrInt, process number 88887.310463/2018-00, International Cooperation Project number 3266, and German Research Foundation (DFG) project 446102036.

DATA AVAILABILITY

No new data were generated or analysed in support of this research.

REFERENCES

Acton C. H., 1996, P&SS, 44, 65
Arlot J.-E., Emelyanov N. V., 2009, A&A, 503, 631
Bosh A. S., Rivkin A. S., 1996, Science, 272, 518
Cooper N. J., Murray C. D., 2004, AJ, 127, 1204
Cooper N. J., Renner S., Murray C. D., Evans M. W., 2015, AJ, 149, 27
Evans M. W., 2001, PhD thesis, Queen Mary University of London,
Everhart E., 1985, An Efficient Integrator That Uses Gauss–Radau Spacings. Springer, Dordrecht, p. 185
French R. G., McGhee C. A., Dones L., Lissauer J. J., 2003, Icarus, 162, 143
Goldreich P., 2003, Icarus, 162, 391
Goldreich P., Rappaport N., 2003, Icarus, 166, 320
Lainey V., Arlot J. E., Vienne A., 2004b, A&A, 427, 371
Lainey V., Duriez L., Vienne A., 2004a, A&A, 420, 1171
McGhee C. A., 2000, PhD thesis, Cornell University
Nicholson P. D., et al., 1996, Science, 272, 509
Quillen A. C., French R. S., 2014, MNRAS, 445, 3959
Renner S., Sicardy B., French R. G., 2005, Icarus, 174, 230
Santana T., Winter O. C., Mourão D. C., 2020, Eur. Phys. J. Spec. Top., 229, 1479
Spitale J. N., Jacobson R. A., Porco C. C., Owen W. M. Jr, 2006, AJ, 132, 692

APPENDIX A: GRAPHICS OF ANTI-ALIGNMENT

In Section 4, we showed how the anti-alignment between Prometheus's and Pandora's orbits, which happens every 6.2 yr, is of the foremost importance. Thus, we computed their orbits starting at different anti-alignments to minimize the difference between our model and the JPL SAT393 at this specific configuration and maximize the time before the subsequent close encounter.

In Fig. A1 we present the graphics showing the difference between BOSS and JPL SAT393 starting at the anti-alignments that occurred after 0.61, 6.9, 13.1, 25.5, 31.7, and 37.9 yr after *Voyager II*'s closest approach to Saturn. These epochs are, respectively, 1982 April, 1988 July, 1994 September, 2007 February, 2013 May, and 2019 July. The anti-alignment that happened 19.3 yr after the referred epoch, in 2000 December, is presented in Fig. 3.

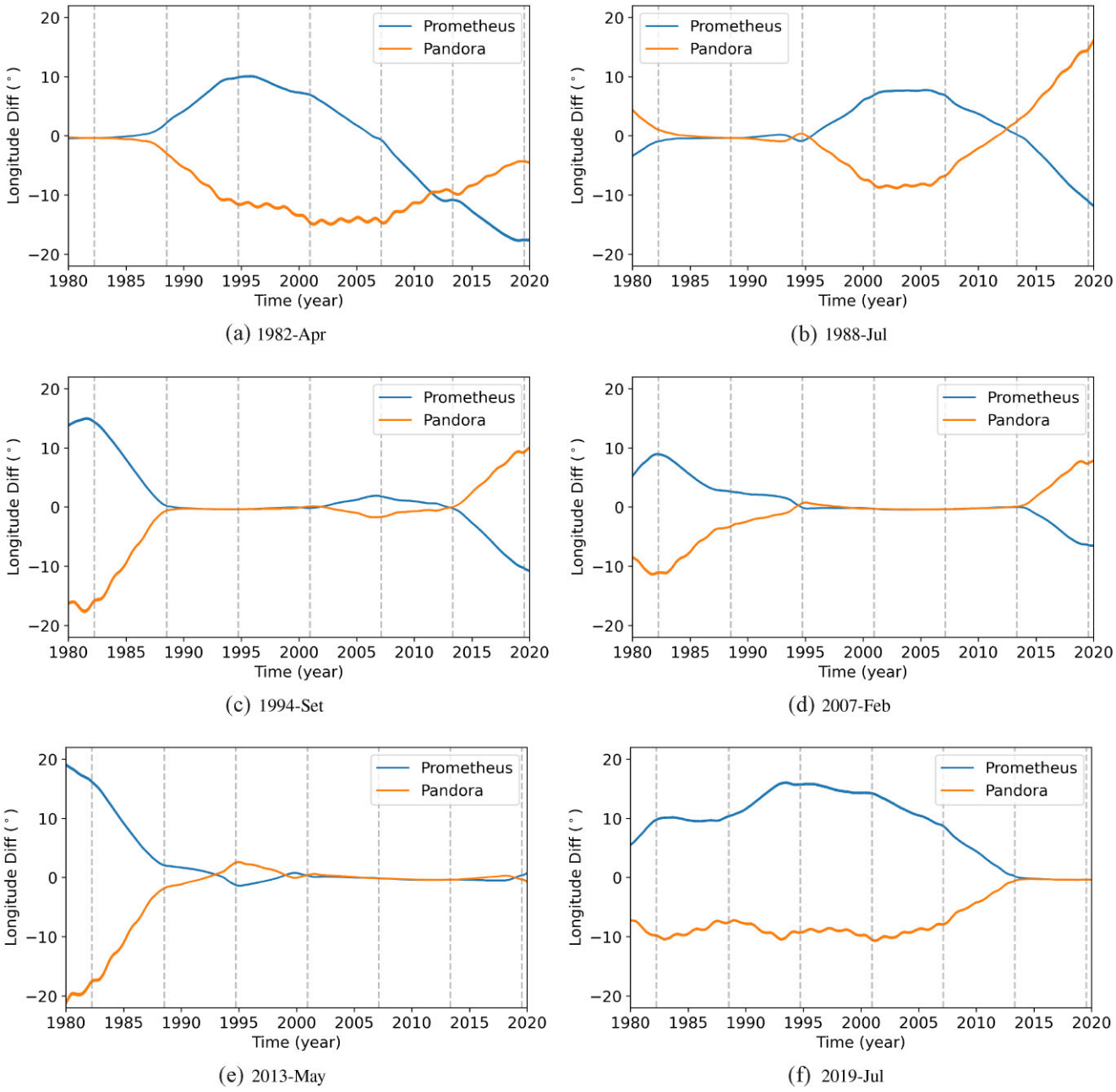

Figure A1. (a–f) Difference in true longitude between BOSS and SAT393 for integrations starting at different anti-alignment epochs.

This paper has been typeset from a TEX/LATEX file prepared by the author.